Semiconductor Physics, Quantum Electronics & Optoelectronics, 2011. V. 14, N 4. P. 470-477.

PACS 61.72.Dd

Transformations of microdefect structure in silicon crystals under the influence of weak magnetic field

T.P. Vladimirova, Ye.M. Kyslovs'kyy, V.B. Molodkin, S.I. Olikhovskii, O.V. Koplak, E.V. Kochelab
G.V. Kurdyumov Institute for Metal Physics, NAS of Ukraine,
36, Vernadsky blvd., 03680 Kyiv, Ukraine

Abstract. Quantitative characterization of complex microdefect structures in annealed silicon crystals (1150 °C, 40 h) and their transformations after exposing for one day in a weak magnetic field (1 T) has been performed by analyzing the rocking curves, which have been measured by a high-resolution double-crystal X-ray diffractometer. Based on the characterization results, which have been obtained by using the formulas of the dynamical theory of X-ray diffraction by imperfect crystals with randomly distributed microdefects of several types, the concentrations and average sizes of oxygen precipitates and dislocation loops after imposing the magnetic field and their dependences on time after its removing have been determined.

Keywords: silicon, supersaturated solid solution, oxygen precipitate, dislocation loop, magnetic field, X-ray diffuse scattering.

Manuscript received 15.05.11; revised manuscript received 19.08.11; accepted for publication 14.09.11; published online 30.11.11.

1. Introduction

Traditionally, external magnetic fields are widely used in semiconductor industry to control behavior of the melt during crystal growth, in particular, the growth of silicon single crystals with a large diameter [1]. The influence of magnetic field on the melt, which reduces the inhomogeneity and melt turbulence and provides the achievement of significant improvement in uniformity of distribution of impurities in grown crystals, is provided due to the action of Lorentz force on moving charged particles – electrons.

Another application of magnetic fields in modern silicon microelectronic industry is to study the interaction of dislocations with impurities such as oxygen or nitrogen [2–6]. This approach is used to lock dislocations in order to prevent their propagation under mechanical stresses arising in technological processes [7, 8]. The importance of these investigations is raised in view of increasing diameters of silicon wafers used in microelectronics and development of defect engineering [9].

For two last decades, the giant and colossal physical and mechanical responses caused by magnetic fields have been discovered in many solids, from oxides of transition metals to the intermetallic compounds and magnetic alloys. The investigations of behavior inherent to various materials in magnetic fields have revealed the existence of significant interactions between spin and crystal lattice, in particular, the manipulation by the spin degree of freedom often leads to structural reconfigurations at the atomic level. The observed significant magnetic responses are in essence the manifestations of structural transitions caused by magnetic field (see reviews [10–12]).

Colossal magneto-physical, thermal, and mechanical phenomena can provide more rapid and energy-saving techniques used in communication systems, storage and processing of information, etc. In particular, as recently shown, the spin degree of freedom for an electron plays a key role in creation of the next generation of electronics, the so-called spintronics [13]. At this forefront of condensed matter physics and technology, the use of interactions between the spin and other, e.g., charge, orbital, and lattice degrees of freedom has both fundamental and applied importance, particularly, in creating the quantum computers [14, 15]. The important fact, which can contribute to rapid integration of new devices into existing systems, is their creation on the basis of silicon crystals which are widely used in modern microelectronics.

© 2011, V. Lashkaryov Institute of Semiconductor Physics, National Academy of Sciences of Ukraine

One of the impressing experimental observations was that the weak magnetic fields can have a significant impact on defect structure and some physical properties of different non-magnetic crystals, including metal-oxide semiconductor structures, oxygen enriched silicon crystals, semiconductors A_2B_6 and A_3B_5, etc. (see reviews [10–12]). Analysis of experimental data shows that the structural changes induced by magnetic field in non-magnetic solids can be interpreted as the disintegration of defect complexes. This disintegration is accompanied by the generation of mobile point defects which are involved in long-term processes and form new defects [10–12].

The observed effects in one of the existing theoretical models are ascribed to the spin-dependent reactions including intrinsic defects and impurities, which are similar to the well-known spin-dependent chemical reactions in liquids and gases [16–20]. The more general model that can describe a wider range of effects in non-magnetic materials, which are caused by imposing the weak magnetic field, is based on the assumption of magnon mechanism for reactions with defects [21, 22]. Nevertheless, theoretical description of the influence of weak magnetic fields on structural transformations in non-magnetic crystals is far from being completed and, in particular, requires detailed quantitative information on the characteristics of small and large clusters involved in these transformations.

X-ray diffraction methods are the most sensitive and informative tool for nondestructive diagnostics of structural changes in crystalline materials and products under various external influences. In recent years, these methods have been enhanced due to the developed theoretical basis of dynamical X-ray diffraction characterization, which allows to reliably determine the quantitative characteristics simultaneously for several types of microdefects with arbitrary radii (from nano- to micrometers) [23]. Thus, the possibility is opened for the adequate interpretation of dynamical diffraction profiles and diffuse scattering intensity distributions measured by high-resolution diffractometers from crystals with a complex defect structure.

The purpose of this paper is to determine the changes of statistical characteristics of microdefects in single-crystalline silicon, namely: concentrations and average sizes of oxygen precipitates and dislocation loops after imposing a weak magnetic field as well as their dependences versus time after its removal, by using the method of high-resolution double-crystal dynamical X-ray diffractometry.

2. Basic theoretical relations

According to the statistical dynamical theory, the diffraction profile measured by the double-crystal diffractometer (DCD) with widely open detector window from the crystal with defects is the sum of coherent (R_{coh}) and diffuse (R_{diff}) components of the crystal reflectivity [23]:

$$R(\Delta\theta) = R_{coh}(\Delta\theta) + R_{diff}(\Delta\theta). \quad (1)$$

Coherent component of the reflectivity is described by the expression:

$$R_{coh}(\Delta\theta) = \left| r_{\mathrm{B}}(y) \right|^2, \quad (2)$$

where the coherent amplitude reflection coefficient in the case of Bragg diffraction geometry is described by the expression [23]:

$$r_{\mathrm{B}}(y) = \varsigma^{1/2}\left[y + i\sqrt{y^2-1}\,\mathrm{ctg}\left(A\sqrt{y^2-1}\right)\right]^{-1}. \quad (3)$$

In the equation (3), the following notations were used:

$$A = \pi t/\Lambda, \quad \Lambda = \lambda\sqrt{\gamma_0|\gamma_{\mathbf{H}}|}/\sigma,$$

$$\sigma^2 = C^2 E^2 \chi_{\mathbf{H}}\chi_{-\mathbf{H}}, \quad \varsigma = \chi_{\mathbf{H}}/\chi_{-\mathbf{H}},$$

$$b = \gamma_0|\gamma_{\mathbf{H}}|^{-1}, \quad \gamma_0 = \sin(\theta_{\mathrm{B}} - \psi),$$

$$\gamma_{\mathbf{H}} = -\sin(\theta_{\mathrm{B}} + \psi),$$

where t is the crystal thickness, Λ – extinction length, C – polarization factor, $E = \exp(-L_{\mathbf{H}})$ – static Debye-Waller factor, $\chi_{\mathbf{H}}$ – Fourier component of the crystal polarizability, b – parameter of diffraction asymmetry, θ_{B} – Bragg angle, ψ – angle between surface and reflecting planes of the crystal. The normalized angular deviation of an imperfect crystal can be written as

$$y = (\alpha - \alpha_0)\sqrt{b}/\sigma, \quad (4)$$

$$\alpha = -\Delta\theta\,\sin(2\theta_{\mathrm{B}}),$$

$$\alpha_0 = [\chi_0 + \Delta\chi_{\mathbf{HH}} + (\chi_0 + \Delta\chi_{00})/b]/2, \quad (5)$$

where $\Delta\theta$ is the angular deviation of the crystal from its exact Bragg reflection position.

The dispersion corrections $\Delta\chi_{\mathbf{HH}}$ and $\Delta\chi_{00}$ in Eq. (5) take into account additional absorption caused by diffuse scattering (DS) from defects. These corrections are complex functions depending on the deviation $\Delta\theta$ ($G = 0$, H):

$$\Delta\chi_{\mathbf{GG}}(\Delta\theta) = P_{\mathbf{GG}}(\Delta\theta) - i\,\mu_{\mathbf{GG}}(\Delta\theta)/K. \quad (6)$$

The absorption coefficients $\mu_{\mathbf{GG}}$ in Eq. (6) are calculated as:

$$\mu_{\mathbf{HH}}(\Delta\theta) \approx \frac{C^2 V}{4\lambda^2}\int \mathrm{d}\mathbf{k}'\,S_{\mathbf{HH}}(\mathbf{q}), \quad (7)$$

$$\mu_{00}(\Delta\theta) \approx b\,\mu_{\mathbf{HH}}(\Delta\theta),$$

where V is the crystal volume, λ – X-ray wavelength. Integration in Eq. (7) is carried out over the plane tangent to the Ewald sphere, and the correlation function $S(\mathbf{q})$ is expressed through the Fourier-components of fluctuating part of the crystal polarizability:

$$S_{\mathbf{GG}'}(\mathbf{q}) = \mathrm{Re}\left\langle \delta\chi_{\mathbf{q}-\mathbf{H}+2\mathbf{G}}\,\delta\chi_{-\mathbf{q}+\mathbf{H}-2\mathbf{G}'}\right\rangle. \quad (8)$$

© 2011, V. Lashkaryov Institute of Semiconductor Physics, National Academy of Sciences of Ukraine

Real parts of dispersion corrections (6) are of the same order of magnitude as their imaginary parts (7), and therefore for numerical calculations one can adopt the approximate relation $P_{\mathbf{GG}} \approx -\mu_{\mathbf{GG}} / K$.

The diffuse component of the crystal reflectivity in the case of Bragg diffraction in single crystals with randomly distributed defects, which is measured using DCD with widely open detector window, can be expressed through the imaginary part of dispersion correction accounting for DS [23]:

$$R_{diff}(\Delta\theta) \approx F_{dyn}(\Delta\theta) \frac{\mu_{\mathbf{HH}}(\Delta\theta)}{2\gamma_0 \mu(\Delta\theta)}, \quad (9)$$

where F_{dyn} is the interference factor of the order of unity, and $\mu(\Delta\theta)$ is the interference absorption coefficient. If randomly distributed defects of several types (α) with size distribution (i) are present in the crystal, then the absorption coefficient related with DS $\mu_{\mathbf{HH}}$ in Eq. (9) can be described by the expression:

$$\mu_{\mathbf{HH}}(\Delta\theta) = \mu_{\mathrm{ds}}(k_0) = \sum_{\alpha} \sum_{\mathrm{i}} \mu_{\mathrm{ds}}^{\alpha\mathrm{i}}(k_0), \quad (10)$$

where $k_0 = K \Delta\theta \sin(2\theta_{\mathrm{B}})$, $K = 2\pi/\lambda$, and $\mu_{\mathrm{ds}}^{\alpha\mathrm{i}}$ are absorption coefficients due to DS from defects of α type with i-th size.

Similarly, if the correlation in defect positions is absent, the exponent of static Debye-Waller factor consists of the sum of contributions from each population of defects $\{\alpha\mathrm{i}\}$:

$$L_{\mathbf{H}} = \sum_{\alpha} \sum_{\mathrm{i}} L_{\mathbf{H}}^{\alpha\mathrm{i}}. \quad (11)$$

Eqs (9) to (11) provide the possibility to describe the angular distribution of the diffuse component in measured rocking curves, which consists of contributions from several types of defects with size distributions. Additionally, Eq. (10) describes the attenuation of the coherent component in rocking curves due to DS from defects.

3. Experimental

X-ray diffraction measurements were carried out with a characteristic $\mathrm{CuK}_{\alpha1}$ radiation from X-ray tube of BSV-29 type with a power of 0.625 kW (25kV×25mA). The high-resolution measurements of RCs for the samples under investigation were performed in the symmetrical Bragg diffraction geometry for Si (111) and (333) reflections by using X-ray optical scheme of DCD with two flat Ge monochromator crystals in a mutually dispersive position.

One of the investigated silicon samples (FZ Si), with sizes 3×2 cm, surface orientation (111), and the diameter 10 cm, was cut from the center of the silicon crystal plate which has been grown by the floating zone method. The sample thickness after lapping and chemo-mechanical polishing was nearly 525 μm. Measurements by using X-ray topography and scanning electron microscopy have not revealed any defects in this sample.

The second investigated sample (Cz Si) was cut from the center of the silicon ingot grown by Czochralski method with a surface orientation (111). The ingot had the p-type conductivity with the resistivity close to 10.5 Ohm·cm, the concentrations of oxygen and carbon impurities were $1.1\times10^{18}\,\mathrm{cm}^{-3}$ and less than $10^{17}\,\mathrm{cm}^{-3}$, respectively. The sample with sizes 10×20 mm after finishing was etched chemically on both sides to a depth 10 μm to the thickness close to 480 μm. This sample was subjected to heat treatment for 40 h at 1150 °C in a sealed silica ampoule in Ar atmosphere.

First of all, the RCs of both samples have been measured before imposing the magnetic field. Then, after the exposition of the samples for one day in the constant weak magnetic field with a strength of 1 T, the RCs have been measured after 1, 5, 8, and 22 days from the moment of switching off the magnetic field.

4. Analysis of measurement results

All the RCs of FZ Si sample that were measured before and after imposing the magnetic field coincide with each other within the limits of statistical errors. This fact indicates that the magnetic field has a little effect on the defect structure of this sample or does not influence it at all. This result is consistent with known literature data on the key role of impurity point defects and their complexes (clusters), which provides mechanisms of the influence of magnetic fields on structural transformations in non-magnetic crystals [10–12]. Since the concentrations of impurities in high-purity silicon crystals grown by the floating-zone method are very low [8], we do not observe any effects of magnetic field on the measured RCs, which are sensitive to a defect structure of the crystal.

At the same time, for Cz Si sample the noticeable differences between all the measured RCs are observed in their central parts (Fig. 1).

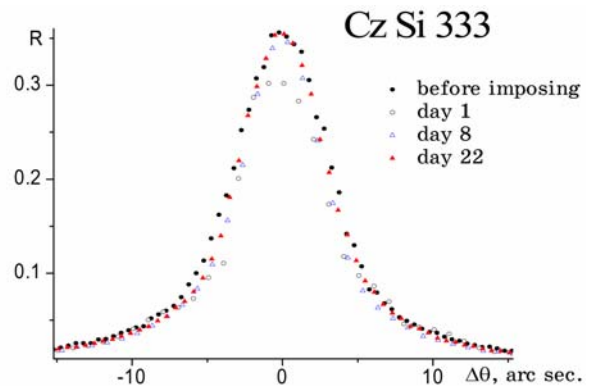

Fig. 1. Experimental RCs (Cz Si 333 reflection, $\mathrm{CuK}_{\alpha1}$ radiation) measured before imposing and after one-day

© 2011, V. Lashkaryov Institute of Semiconductor Physics, National Academy of Sciences of Ukraine

exposition in the weak magnetic field with subsequent ageing in air during 1, 8, and 22 days.

This specific form of RCs requires a careful choice of an adequate model of the defect structure of the sample and accurate fit of the measured RCs during their treatment. It is known that silicon crystals grown by the Czochralski method contain usually several types of microdefects (oxygen precipitates, stacking faults or dislocation loops of interstitial type) with size distributions from nano- to micrometers [2]. These distributions evolve during thermal treatments at elevated temperatures due to interaction of oxygen impurity and intrinsic point defects.

In the model of microdefect structure of Cz Si sample, which was used in the treatment of the measured RCs, it was assumed that three types of microdefects are present in the crystal, namely: disc-shaped and spherical precipitates of radius R_P (and thickness h_P for disc-shaped precipitates), and concentration n_P, as well as circular dislocation loops of radius R_L and concentration n_L. When analyzing the measured RCs, also contribution of thermal DS and influence of instrumental factors were taken into account [23]. The fit quality was estimated using an ordinary (R) and weighted (R_w) reliability factors.

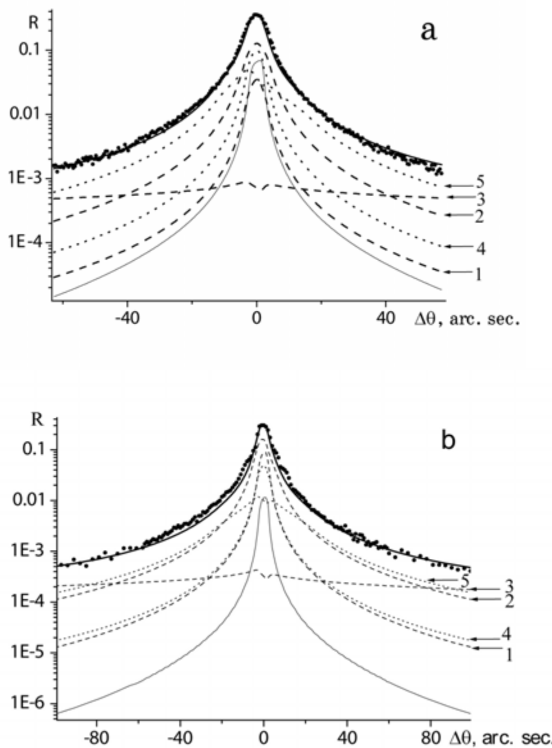

Fig. 2. Experimental and calculated RCs (333 reflection, CuK$_{\alpha1}$ radiation) measured before imposing (a) and one day after removing (b) the weak magnetic field from Cz Si crystal exposed during one day (markers and solid lines, respectively). The contributions of coherent scattering and DS from dislocation loops of different sizes (1, 2, 3), and disc-shaped (4) and spherical (5) oxygen precipitates (see Table 1) are described by thin solid, dashed, and dotted lines, respectively.

The results of X-ray diffraction characterization of the annealed Cz Si sample before and after imposing a weak magnetic field are shown in Table 1 (see also Fig. 2). The values of defect characteristics have been determined by fitting all RCs with ordinary and weighted reliability factors not exceeding R = 10% and R_w = 15%, respectively.

It should be remarked that the possibility of the simultaneous determination of the characteristics of three types of microdefects has been realized due to self-consistent description of coherent and diffuse components in the RCs. Besides, an important factor for achieving uniqueness and increasing diagnostic accuracy was the self-consistency of contributions of coherent and diffuse RCs components both at the tails and in the total reflection range. For this purpose, in particular, it was necessary to take into account the existence of a wide spread of dislocation loop radii from tens to hundreds of nanometers. The reliability of characterization was enhanced also due to the account for the presence of antisymmetric components in DS intensity distributions from oxygen precipitates and dislocation loops.

As can be seen from the results of X-ray dynamical diffraction characterization (Table 1), the sufficiently significant transformations of microdefect structure in the Cz Si sample under the influence of the weak magnetic field have occurred. They are exhibited in the decrease of average sizes of oxygen precipitates (Fig. 3) and corresponding decrease of oxygen concentration in the disc-shaped and spherical oxygen precipitates C_{O}^{P} (Fig. 4). Simultaneously, the average radii of large dislocation loops (Fig. 5) and concentration of silicon atoms in them C_{i}^{L} has been increased (Fig. 6). Then, after removing the magnetic field, the defect structure was relaxed, i.e., the microdefect characteristics have been gradually recovered to their initial values that existed prior to imposing the magnetic field (see Figs 3 to 6, where marker sizes correspond to error bars).

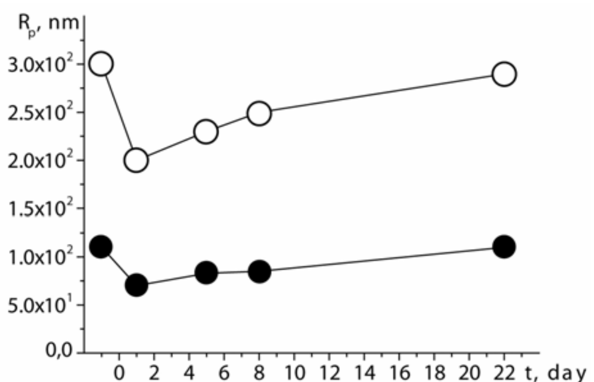

Fig. 3. Dependences of the radii of disc-shaped and spherical oxygen precipitates (filled and empty markers, respectively) in

© 2011, V. Lashkaryov Institute of Semiconductor Physics, National Academy of Sciences of Ukraine

the Cz Si crystal versus time after removing the magnetic field. Marker sizes correspond to error bars.

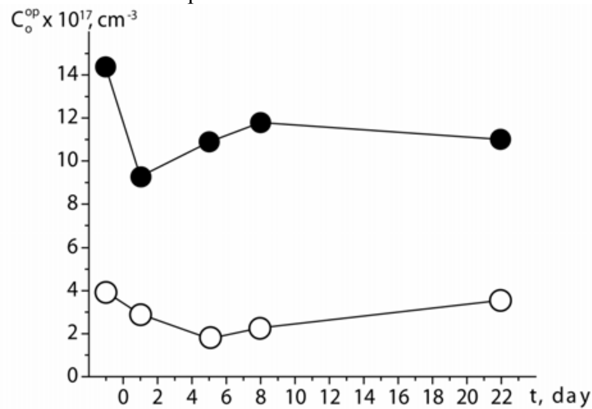

Fig. 4. Dependences of concentrations of oxygen atoms in disc-shaped and spherical oxygen precipitates in Cz Si crystal (filled and empty markers, respectively) versus time after removing the magnetic field for 333 reflection.

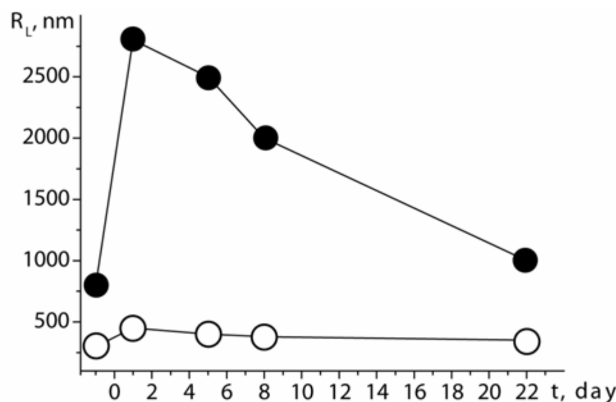

Fig. 5. Dependences of radii of large and medium dislocation loops (filled and empty markers, respectively) in Cz Si crystal versus time after removing the magnetic field.

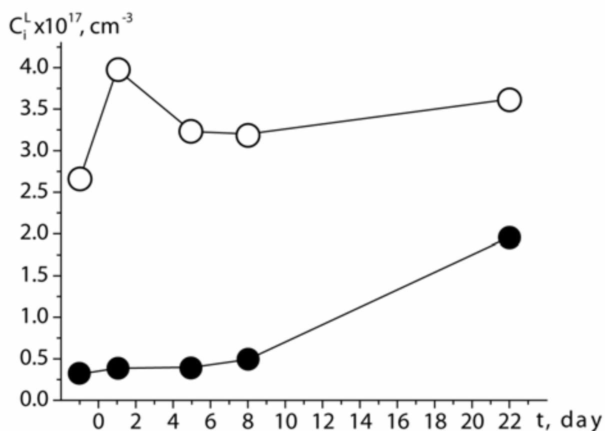

Fig. 6. Dependences of concentrations of silicon atoms in large- and medium-size dislocation loops (filled and empty markers, respectively) versus time after removing the magnetic field for 333 reflection.

5. Discussion

The intrigue of the observations described above is that the weak magnetic field with the induction of 1 T can transfer to a paramagnetic particle only the energy of $\sim\mu_B B \sim 10^{-4}$ eV (μ_B is the Bohr magneton) [10 – 12], which is about two orders of magnitude smaller than the mean energy of thermal fluctuations at room temperature $\sim k_B T \sim 10^{-2}$ eV (k_B is the Boltzmann constant, T – absolute temperature) and four orders smaller than the activation energy for joining the atom to the cluster $E_{act} \sim 1$ eV. For this reason, it is not clear which physical mechanism is responsible for the observed structural changes. Despite the recently published first attempts of the theoretical interpretation of physical phenomena, including structural changes, in non-magnetic crystals under the influence of weak magnetic fields [16 – 22], the search for an adequate theoretical model to describe observed phenomena remains urgent.

In particular, when developing the kinetic models of defect clustering in non-magnetic crystals under the influence of magnetic field [19] and its application to the case of silicon crystals grown by the Czochralski method, the important circumstance should be taken into account that these crystals are very supersaturated solid solutions of oxygen in silicon [8]. During cooling in the growth process and after various thermal treatments, the oxygen precipitates are formed due to decomposition of these solutions, and simultaneously dislocation loops are formed because of accompanying rise and decomposition of the supersaturated solid solution of interstitial silicon atoms [8, 9]. Very often, the decomposition processes are not completed fully, and the metastable defect structure is "frozen" in the crystal, as it is observed in the case of the investigated Cz Si sample.

One can suppose that during exposition in a magnetic field this defect structure transits to another metastable state due to its interaction with the spin degree of freedom of defects. This process of the transition is characterized by detaching oxygen atoms from the precipitates and attaching excess silicon interstitial atoms to existing dislocation loops, what leads to the decrease of mean average radius of oxygen precipitates and increase of average radius of dislocation loops (Table 1). After removal of the magnetic field, a gradual recovery of the metastable defect structure to its initial state occurs during several weeks under the influence of thermal fluctuations (Figs. 4 to 6).

To describe in details the evolution of the defect structure in the silicon crystal grown by the Czochralski method and, in particular, its transformation under the influence of weak magnetic fields, a complicated system of coupled equations of chemical reactions, differential Fokker-Planck equations, and mass conservation laws

© 2011, V. Lashkaryov Institute of Semiconductor Physics, National Academy of Sciences of Ukraine

for point defects should be solved numerically [24 – 26]. Nevertheless, some laws of the behavior of such complicated physical systems can be established by using the dimensional analysis of these equations and investigation of the relevant characteristic constants [25, 27].

One of important parameters that characterizes the process of oxygen precipitation in silicon and is closely related with the average radius of oxygen precipitates is their critical radius [24 – 26]. If the radius of an oxygen precipitate formed due to stochastic processes of attachment of oxygen atoms exceeds some critical value, it continues to grow, while a precipitate with a smaller radius dissolves. When interaction of the oxygen precipitate with interstitial silicon atoms and vacancies is taken into account, the critical radius of the oxygen precipitate has the form [25]:

$$R_P^{cr} = \frac{2\sigma u V_p}{k_B T \ln\left(S_O S_i^{-\gamma_i} S_v^{\gamma_v}\right) - 6\mu\delta\varepsilon u V_p},$$

$$u = \left(1+\gamma_i x + \gamma_v x\right)\left(\frac{1+\varepsilon}{1+\delta}\right), \qquad (12)$$

where σ is the surface energy of the boundary between oxygen precipitates and silicon matrix, V_p is volume of the SiO_x molecule, $S_O = C_O / C_O^{eq}$, $S_i = C_i / C_i^{eq}$, and $S_v = C_v / C_v^{eq}$ are supersaturations of interstitial oxygen and silicon atoms as well as vacancies, respectively, C_O, C_i, C_v and C_O^{eq}, C_i^{eq}, C_v^{eq} – actual and equilibrium concentrations of interstitial oxygen and silicon atoms, and vacancies, respectively, γ_i and γ_v – ratios of amounts of emitted interstitial silicon atoms and absorbed vacancies to the amount of oxygen atoms attached to the precipitate, μ is shear modulus of silicon, ε and δ are bulk and linear strains at the boundary between precipitate and matrix, respectively.

Similarly, for dislocation loops of the interstitial type there exists a characteristic size, namely, the critical radius R_L^{cr} that can be found as a solution of the transcendental equation [25]:

$$\left.\frac{R_L/b}{\ln\left(R_L/b\right)+c}\right|_{R_L=R_L^{cr}} = \frac{\mu V_m}{2\pi(1-\nu)}\left[k_B T \ln\left(S_i S_v^{-\gamma_v^*}\right) - 2\varepsilon_{sf} V_m / b\right]^{-1}, \qquad (13)$$

where the constant $c = 2.96$, b is the module of Burgers' vector , ν – Poisson ratio, ε_{sf} – surface energy of stacking fault, V_m – volume of Si atom.

By using the determined average radii of oxygen precipitates and dislocation loops (Table 1) and the expressions for the corresponding critical radii of these microdefects (12) and (13), one can determine the parameters of supersaturation of point defects

Table 1. Characteristics of oxygen precipitates and dislocation loops in Cz Si crystal before and after imposing the magnetic field as determined from RCs for 333 reflection. The fit quality was estimated with ordinary and weighted reliability factors not exceeding R = 10% and R_w = 15%, respectively.

Data	R_L, nm	n_L, cm^{-3}	$C_i^L \times 10^{17}$, cm^{-3}	R_P, nm	h_P, nm	n_P, cm^{-3}	$C_O^P \times 10^{17}$, cm^{-3}
Before	800	1.0×10^9	0.3	110	6.2	1.3×10^{11}	14.3
imposing	300	6.0×10^{10}	2.7	300	–	8.0×10^7	3.9
field	0.5	4.0×10^{18}	492.4				
∑ =			495.4				18.2
	2800	1.0×10^8	0.4	70	5.2	2.5×10^{11}	9.3
Day 1	450	4.0×10^{10}	4.0	200	–	2.0×10^8	2.9
	0.5	1.5×10^{18}	184.7				
∑ =			189.1				12.2
	2500	1.2×10^8	0.4	83	5.4	2.0×10^{11}	10.9
Day 5	400	4.1×10^{10}	3.2	230	–	8.0×10^7	1.8
	0.5	1.5×10^{18}	184.7				
∑ =			188.3				12.7
	2000	2.5×10^8	0.5	85	5.6	2.0×10^{11}	11.8
Day 8	380	4.5×10^{10}	3.2	250	–	8.0×10^7	2.3
	0.5	1.5×10^{18}	184.7				
∑ =			188.4				14.1
	1000	1.0×10^9	2.0	110	6.2	1.0×10^{11}	11.0
Day 22	350	6.0×10^{10}	3.6	290	–	8.0×10^7	3.6
	0.5	1.5×10^{18}	184.7				
∑ =			190.3				14.6

Table 2. Supersaturation parameters for point defects in Cz Si crystal before imposing the magnetic field and one day after removing it ($A = S_i S_v^{\gamma_v^*}$, $B = S_O S_i^{-\gamma_i} S_v^{\gamma_v}$).

Data	R_L, nm	ln A	A	R_P, nm	ln B	B
Before imposing field	800	0.29	1.34	110	1.671	5.32
	300	0.68	1.97	300	1.660	5.26
Day 1	2800	0.10	1.11	70	1.681	5.37
	450	0.48	1.61	200	1.664	5.28

(interstitial oxygen and silicon atoms, and vacancies) and their corresponding equilibrium concentrations before and after imposing the magnetic field (see Table 2). These values, in turn, can be used to estimate changes in activation energies of point defects and to analyze the driving forces of structural changes at the imposition of a weak magnetic field on silicon crystals.

It should be also remarked that after switching off the magnetic field transformation of the defect structure in the investigated Cz Si sample is continued, and its gradual and non-uniform relaxation occurs to the state that preceded the imposition of the magnetic field (Figs 3 to 6). The growth of oxygen precipitates during this relaxation is accompanied by decrease in the oxygen concentration and increase in the concentration of interstitial silicon atoms due to their emission from growing oxygen precipitates and due to shrinkage of large dislocation loops. Since two interacting supersaturated solid solutions of interstitial oxygen and silicon atoms coexist in the silicon crystal and, according to Eq. (12), the increase of supersaturation by interstitial silicon atoms inhibits the growth of oxygen precipitates, whereas, according to Eq. (13), the same supersaturation slows the shrinkage of dislocation loops. Thereof, one can conclude that the critical radii of oxygen precipitates and dislocation loops and the corresponding average radii of these microdefects will drift during the relaxation over corresponding hypersurfaces in a space of concentrations of point defects. At the same time, both microdefect radii and concentrations of interstitial oxygen and silicon atoms can have wave-like time dependences (Figs 4 to 6).

In conclusion, it should be emphasized that the obtained results suggest the possibility of an effective application of the dynamical high-resolution X-ray diffraction measurements, which allow reliable determining the quantitative characteristics simultaneously of several types of microdefects, for the quantitative characterization of structural changes in non-magnetic crystals under the influence of weak magnetic fields. In turn, information obtained in this way can contribute to the creation of adequate models of such structural transformations.

6. Summary and conclusions

The measurements of RCs of the silicon single crystal annealed at 1150 °C for 40 h before superposition of a weak magnetic field (1 T) and after exposure in this field for one day as well as after certain time intervals have been carried out by using high-resolution double-crystal X-ray diffractometer. Based on characterization results, which have been obtained using formulas of the dynamical theory of X-ray diffraction in imperfect crystals with randomly distributed microdefects of several types, the change of average sizes of oxygen precipitates and dislocation loops after imposing the weak magnetic field has been determined as well as their dependence on the time passed after the removal of the magnetic field.

It has been established that during aging the silicon crystal in a magnetic field transformation of its metastable defect structure to another metastable state occurs due to its interaction with the spin degree of freedom of defects. This transformation is characterized by removing oxygen atoms from the precipitates and attaching excess interstitial silicon atoms to existing dislocation loops. These processes lead to decrease of the average radius of oxygen precipitates and increase of the average radius of large dislocation loops. After removal of the magnetic field, a gradual recovery of the defect structure to its initial metastable state under the influence of thermal fluctuations occurs for several weeks.

The obtained results indicate promising applications of the dynamical X-ray diffractometry for quantitative characterization of complicated structural transformations, which occur under the influence of magnetic fields in non-magnetic crystals, including silicon single crystals grown by the Czochralski method.

This work was performed with the financial support of the National Academy of Sciences of Ukraine (Contract No. 3.6.3.13−7/10−D).

References

1. Th. Kaiser, K.W. Benz, Floating-zone growth of silicon in magnetic fields. III. Numerical simulation // *J. Cryst. Growth,* **183**(4), p. 564-572 (1998).
2. M.V. Badylevich, U.L. Iunin, V.V. Kveder, V.I. Orlov, Yu.A. Ossipyan, Influence of magnetic field on unlocking stress and mobility of individual dislocations in silicon // *Zhurnal eksperiment. teor. fiziki,* **124**, No.3(9), p. 664-669 (2003), in Russian.
3. M.V. Badylevich, V.V. Kveder, V.I. Orlov, Yu.A. Ossipyan, Spin-resonant change of unlocking stress for dislocations in silicon // *Phys. status solidi* (*c*), **2**, p. 1869-1872 (2005).
4. N.N. Novikov, B.D. Patsay, V.M. Tsmots, P.G. Litovchenko, Yu.V. Pavlovskii, M.M. Luchke-vych, Influence of high temperature treatment on structural and magnetic changes in silicon crystals // *Zhurnal fiz.doslidzhen'* **9**(4), p. 319-324 (2005), in Ukrainian.
5. V.A. Makara, L.P. Steblenko, Yu.L. Kolchenko, S.M. Naumenko, I.P. Lisovsky, D.O. Mazunov, Yu.Yu. Mokliak, Effect of weak magnetic field on structural arrangement of extrinsic oxygen atoms and mechanical properties of silicon monocrystals // *Semiconductor Physics, Quantum Electronics & Optoelectronics,* **9**(2), p. 1-3 (2006).
6. D.R. McCameyl, G.W. Morley, H.A. Seipel, L.C. Brunel, J. van Tol, C. Boehme, Spin-dependent processes at the crystalline Si-SiO_2 interface at high magnetic fields // *Phys. Rev. B,* **78**(4), 045303 (2008).

© 2011, V. Lashkaryov Institute of Semiconductor Physics, National Academy of Sciences of Ukraine

7. K. Jurkschat, S. Senkader, P.R. Wilshaw, D. Gambaro, R.J. Falster, Onset of slip in silicon containing oxide precipitates // *J. Appl. Phys*. **90**(7), p. 3219-3225 (2001).
8. A. Borghesi, B. Pivac, A. Sassella, A. Stella, Oxygen precipitation in silicon // *J. Appl. Phys.* **77**(9), p. 4169-4244 (1995).
9. T. Sinno, E. Dornberger, W. von Ammon, R.A. Brown, F. Dupret, Defect engineering of Czochralski single-crystal silicon // *Mater. Sci. Eng.* **28**, p. 149-198 (2000).
10. R.B. Morgunov, Spin micromechanics in physics of plasticity // *Physics-Uspekhi* **174**(2), p. 131-153 (2004).
11. O.I. Golovin, Magnetoplasticity of solids // *Fizika Tverd. Tela,* **46**(5), p. 769-803 (2004), in Russian.
12. A.L. Ivanovskii, Magnetic effects in non-magnetic sp-materials induced by sp-impurities and defects // *Physics-Uspekhi,* **177**(10), p. 1083-1105 (2007).
13. M.E. Flatté, Solid-state physics: Silicon spintronics warms up // *Nature,* **462**, p. 419-420 (2009).
14. R.W. Keyes, Effects of the magnetic field in quantum computing with silicon // *J. Phys.: Condens. Matter.* **17**(23), p. V9-V11 (2005).
15. M.J. Calderón, B. Koiller, S. Das Sarma, Magnetic-field-assisted manipulation and entanglement of Si spin qubits // *Phys. Rev. B,* **74**(8), 081302(R) (2006).
16. V.I. Belyavsky, M.N. Levin, Spin effects in defect reactions // *Phys. Rev. B,* **70**(10), 104101 (2004).
17. A.L. Buchachenko, Influence of magnetic field on mechanics of non-magnetic crystals: origin of the magnetoplastic effect // *Zhurnal eksperiment. teor. fiziki,* **129**(5), p. 909-913 (2006), in Russian.
18. A.L. Buchachenko, Magnetoplasticity of diamagnetic crystals in microwave fields // *Zhurnal eksperiment. teor. fiziki,* **132**, No.3(9), p. 673-679 (2007), in Russian.
19. A.L. Buchachenko, Physical kinetics of magnetoplasticity in diamagnetic crystals // *Zhurnal eksperiment. teor. fiziki,* **132**, No.4(10), p. 827-830 (2007), in Russian.
20. R.B. Morgunov, A.L. Buchachenko, Magneto-plasticity and magnetic memory in diamagnetic solids // *Zhurnal eksperiment. teor. fiziki,* **136**(3), p. 505-515 (2009), in Russian.
21. V.I. Belyavsky, Yu.V. Ivankov, M.N. Levin, Magnon mechanism of reactions between defects in solids // *Fizika Tverd. Tela,* **48**(7), p. 1255-1259 (2006), in Russian.
22. V.I. Belyavsky, M.N. Levin, N.J. Olson, Defect-induced lattice magnetism: Phenomenology of magnetic-field-stimulated defect reactions in nonmagnetic solids // *Phys. Rev. B*, **73**(5), 054429 (2006).
23. V.B. Molodkin, S.I. Olikhovskii, E.N. Kislovskii, T.P. Vladimirova, E.S. Skakunova, R.F. Seredenko, B.V. Sheludchenko, Dynamical theoretical model of the high-resolution double-crystal x-ray diffractometry of imperfect single crystals with microdefects // *Phys. Rev. B,* **78**(22), 224109 (2008).
24. M.M. Belova, M.N. Moskal'kov, A.Ye. Rudich, S.Y. Olikhovsky, E.V. Kochelab, Modeling the evolution of microdefect system in crystalline supersaturated solid solution. I. Evolution equations and conservation laws // *Metallofizika Noveishie Technologii,* **29**(4), p. 427-450 (2007), in Russian.
25. S.I. Olikhovskii, M.M. Belova, M.N. Moskal'kov, Yu.A. Belov, A.Ye. Rudich, E.V. Kochelab, Modeling the evolution of microdefect system in crystalline supersaturated solid solution. II. Dimensional analysis of evolution equations and diffusion // *Metallofizika Noveishie Technologii,* **29**(5), p. 649-662 (2007), in Russian.
26. M.M. Belova, M.N. Moskal'kov, Yu.A. Belov, A.Ye. Rudich, S.I. Olikhovsky, E.V. Kochelab, Modeling the evolution of microdefect system in crystalline supersaturated solid solution. III. Numeric calculations // *Metallofizika Noveishie Technologii,* **29**(6), p. 727-742 (2007), in Russian.
27. Ye.M. Kyslovskyy, T.P. Vladimirova, S.I. Olikhovskii, V.B. Molodkin, E.V. Kochelab, R.F. Seredenko, Evolution of the microdefect structure in silicon at isothermal annealing as determined by X-ray diffractometry // *Phys. status solidi* (*a*), **204**(8), p. 2591-2597 (2007).

© 2011, V. Lashkaryov Institute of Semiconductor Physics, National Academy of Sciences of Ukraine